Aerospace Science and Technology 148 (2024) 109107

Contents lists available at ScienceDirect

Aerospace Science and Technology

journal homepage: www.elsevier.com/locate/aescte

Transient plasma enhanced combustion of solid rocket propellants

Caleb Medchill [b,c], Armando A. Perezselsky [c], Andrew Cortopassi [c], Alejandro L Briseno [c], Chris Brophy [d], Stephen B. Cronin [a,b,*]

[a] Department of Chemistry, University of Southern California, Los Angeles, CA 90089, United States
[b] Ming Hsieh Department of Electrical Engineering, University of Southern California, Los Angeles, CA 90089, United States
[c] Aerospace Corporation, El Segundo, CA 90245, United States
[d] Naval Postgraduate School, Monterey, CA 93943, United States

ARTICLE INFO

Editor: Suresh Menon

Keywords:
Plasma
Propellant
Energetics
Solid
Propulsion
Throttleable

ABSTRACT

We demonstrate the use of nanosecond pulse transient plasma (NPTP) to improve the control (and acceleration) of the combustion of solid rocket propellants. Here, we fabricate end-burning propellant samples (i.e., grains) with a co-axial center wire electrode using hydroxyl terminated polybutadiene (HTPB), isodecyl pelargonate (IDP), modified diphenyl diisocyanate (MDI), and ammonium perchlorate (AP) as the fuel, plasticizer, curative, and oxidizer, respectively. High voltage (20 kV) nanosecond pulses (20 nsec) produce a streamer discharge that provides electronic throttling of the solid rocket propellant. These studies are carried out over a wide range of oxidizer mass fractions, including those considered insensitive munitions (IM). In addition, real time imaging is performed characterizing the plasma-formation, evolution of the ignition process, and plasma enhanced flame-fuel coupling. We believe the plasma-based mechanisms of enhancement are 3-fold: 1.) The plasma provides highly energetic electrons that drive new chemical reaction pathways via highly reactive atomic species such as H, O, and Cl, 2.) The plasma sputters chunks of the solid fuel material up into the flame where it is combusted, producing an agitated flame profile. 3.) The plasma provides increased turbulence and multi-scale mixing due to hydrodynamic effects (i.e., ionic winds), which further improves the combustion process. Having *electronic* control of the burn rate introduces the ability to "throttle" solid rocket motors and introduce new flight profile options beyond a pre-selected profile such as the typical boost-sustain profile. While we are unable to quantify the burn rate or thrust from these relatively simple observations, we observe clear evidence of the effect of the plasma on the combustion of these solid rocket fuels even at high oxidizer content.

Introduction

Electrical ignition and control of solid rocket propellants was proposed many years ago[1] and more recent studies have shown some ability to increase the specific impulse efficiencies with electrical solid propellants [2]. The incorporation of "electronic" control over the burn rate enables the ability to adjust the power output of the solid propellant motor, opening up new possibilities for flight profiles that go beyond a predetermined option, like the standard boost-sustain profile. For example, a simple burn-glide-burn-glide flight profile could significantly extend the range of a given propellant. Other attempts to achieve electronic throttling include embedding highly conductive wires in the solid propellant, laser-assisted combustion, and using microwave electromagnetic radiation to accelerate burn rates [3,4]. However, it should be noted that these previous attempts represent thermal equilibrium approaches (i.e., same reaction pathways), while the work reported here utilizes a non-thermal plasma with electron temperatures as high as 40,000 K, which enables new chemical pathways and reaction mechanisms to be achieved.

It is worth noting that transient plasma-enhanced combustion has been demonstrated in natural gas combustion [5–13], gasoline engines [14–18], as well as the combustion of "green" (i.e., carbon-free) fuels, such as ammonia [19–21]. In addition, transient plasma has been demonstrated as an effective and energy efficient technology for a variety of applications including reduced ignition delays in a range of engines such as internal combustion engines (ICE) and pulse detonation engines (PDE), reduction of particulate emissions from diesel and other sources, and improving flame holding performance [10,22-25]. For example, PDE discharges in a flowing system have been shown to reduce the ignition delays in fuel/air mixtures by factors of approximately 5X,

* Corresponding author.
E-mail address: scronin@usc.edu (S.B. Cronin).

https://doi.org/10.1016/j.ast.2024.109107
Received 20 October 2023; Received in revised form 19 March 2024; Accepted 31 March 2024
Available online 4 April 2024

and up to 9X for fuel/oxygen mixtures. These previously observed benefits are believed to be due in part to the local production of ozone, which is a well-known flame accelerant, produced by nanosecond pulse technology that is responsible for transient plasma generation. However, transient plasma has not yet been used to enhance solid rocket propellants.

In the work presented here, end-burning propellant grains are fabricated using a 1.37″ (inner) diameter stainless steel cylinder with a 0.025″ diameter coaxial center wire electrode, as illustrated in Fig. 1. The volume between the center wire and outer cylinder is filled with a mixture of hydroxyl-terminated polybutadiene (HTPB), ammonium perchlorate (AP), isodecyl pelargonate (IDP) and modified diphenyl diisocyanate (MDI), which act as the fuel, oxidizer, plasticizer, and curative, respectively. The ratios were 0.147 g of MDI, 0.15 to 0.38 g of IDP, and 0.15 g to 8.67 g of AP per gram of HTPB. The oxidizer percentage was determined by using the total mass of HTPB, IDP and MDI. A complete list of mass ratios in all of the fuel mixtures are given in Table S1 of the Supporting Information document. The fuel, oxidizer, curative and plasticizer were mixed using resonant acoustic mixing (Resodyn LabRAM system). Each mixture was then held under vacuum to remove any air bubbles. The propellant mixture was then poured into the stainless steel shell and left to cure for at least 72 h. The mixture was set to cure in the cylindrical test cell which, as mentioned above, consists of a 1.37″ diameter steel pipe with a 0.025″ diameter coaxially configured center wire that enables plasma discharge.

Fig. 2a shows a schematic diagram of our experimental setup in which the high voltage nanosecond pulse electronics are connected to the coaxial plasma reactor with an end burner grain. Figs. 2b and c show photographs of the test cell during combustion with and without plasma discharge. 20 kV nanosecond pulses were delivered at a variable rate between 0 and 10 kHz. Increasing the frequency to 10 kHz generates a much higher observable burning rate of the fuel mixture, which is tunable by varying the pulse repetition rate and, hence, plasma density. Here, we can see a dramatic increase in the flame height during plasma discharge. Although somewhat qualitative, these results demonstrate our ability to electronically-throttle the combustion rate of solid rocket engines.

Fig. 3a shows time series images of an end burner grain prepared with 25 % oxidizer (i.e., ammonium perchlorate). In this time series, the plasma (discharged at a rate of 10 kHz) is turned on at $t = 1$ s and turned off at $t = 41.4$ s. For this fuel mixture (i.e., 25 % AP), the flame takes approximately 30 s to reach steady state flame conditions with the plasma on. After the plasma is turned off at $t = 41.4$ s, the flame quickly dies within a few seconds. This "on" in 30 s and "off" in 5 s demonstrates the electronic throttlability of this plasma-enhanced solid rocket combustion. With the plasma on, the flame appears to have a much more agitated fame profile than with the plasma off. We believe this is due to the plasma sputtering solid material up into the flame where it combusts 0.5″ – 1″ above the solid rocket fuel. The right images in Fig. 3a were taken with a 430 nm band pass filter, which indicates the location of short-lived CH intermediate radical species produced in the combustion process. These images provide additional insight into the plasma-enhanced combustion process and chemical reaction pathways. More specifically, it is remarkable that this CH combustion chemistry propagates upwards 1″ above the plasma discharge zone and is almost completely absent with the plasma off. It is interesting to note that the plasma-flame coupling extends 1″ above the solid rocket propellant surface and that the flame-propellant coupling is significantly enhanced with the plasma discharge. The full videos (both filtered and unfiltered) of this burn are available in the Supplemental Information. Figs. 3b and c show the integrated intensity collected from the unfiltered and 430 nm-filtered videos plotted as a function of time for 25 % oxidizer burn mixture. Here, a 30 second time interval is needed to reach steady state flame conditions with the plasma on. We also observe an abrupt drop in intensity (i.e., luminescence) after the plasma is turned off at $t = 41.4$ s.

Fig. 4a shows the (CH) filtered and unfiltered time series images

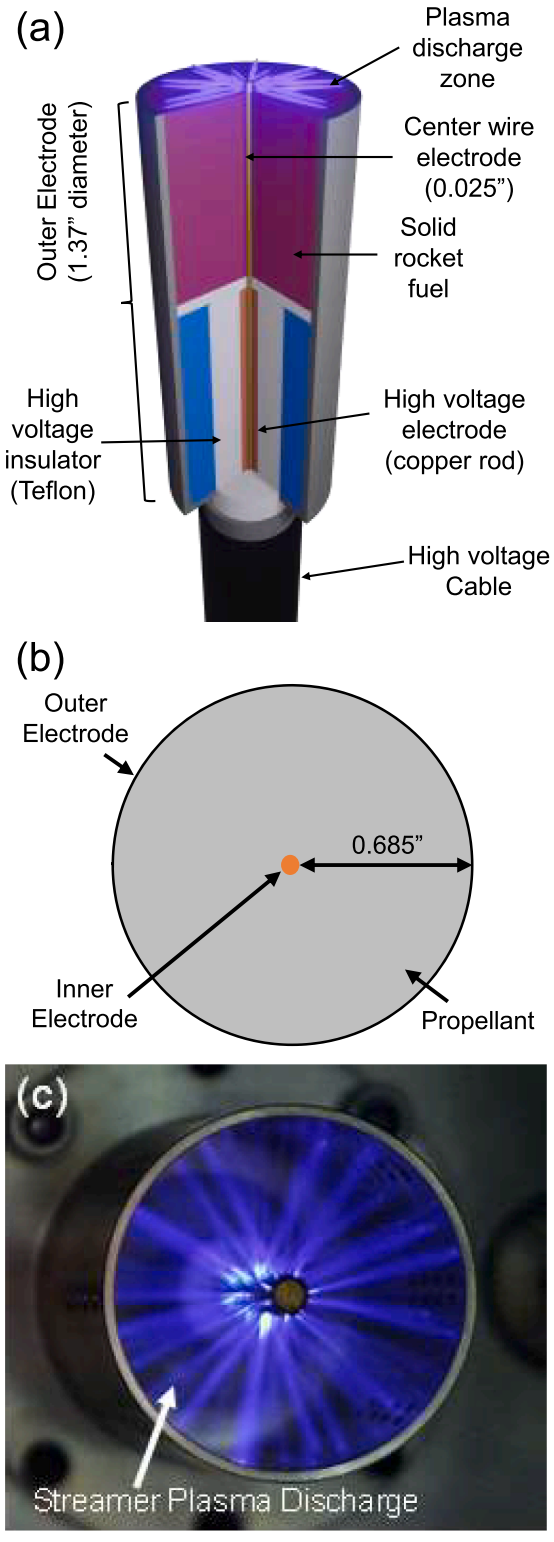

Fig. 1. (a,b) Cross-sectional diagrams of our initial test configuration consisting of a 1.37″ diameter end-burning propellant sample. (c) Photograph of the transient plasma discharge formed by our high voltage nanosecond pulse approach.

taken of the plasma-enhanced end burner grain prepared with 35 % oxidizer. Here, the flame reaches its steady state conditions (i.e., magnitude) after approximately 15 s, which is considerably shorter than that of the 25 % oxidizer grain, as expected, reflecting the higher

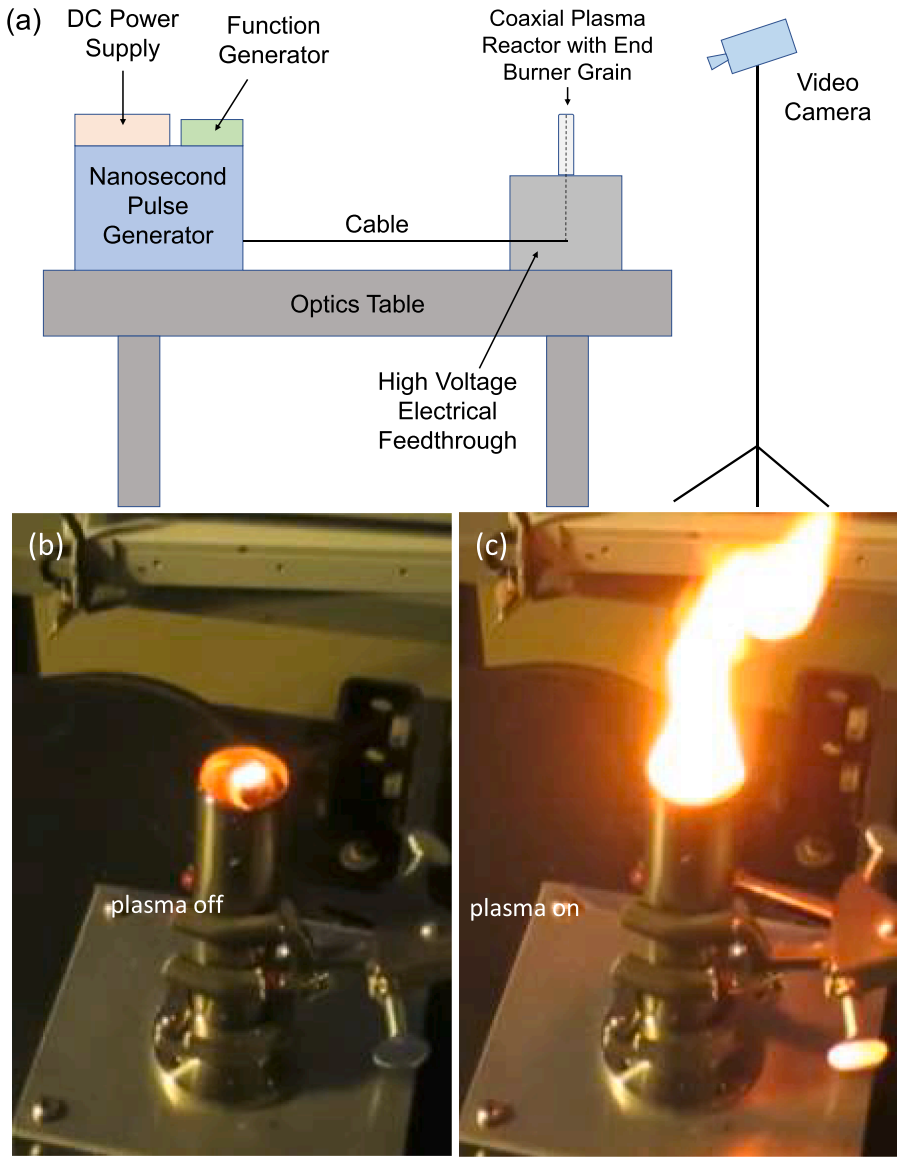

Fig. 2. (a) Schematic diagram of our experimental setup in which the high voltage nanosecond pulse electronics are connected to the coaxial plasma reactor with an end burner grain. Photographs of the test cell during combustion (b) without and (c) with plasma discharge. The fuel mixture contains 30 % oxidizer (ammonium perchlorate). This is an end burner open to atmosphere system. The center wire caries the high voltage while the outer shell acts as the ground. (c) Increasing the frequency to 5 kHz generates a much higher observable burning rate of the fuel mixture, which can be tuned by controlling the pulse repetition rate of the plasma.

oxidizer content. The combustion is visually confirmed to be at steady state before turning the plasma off. After the plasma is turned off at $t =$ 22 s, the flame becomes fully extinguished after approximately 5 s or less. Immediately after turning off the plasma ($t = 22$ s), however, the CH emission ceases immediately in the absence of the plasma. We believe the mechanism of the plasma enhancement of the combustion process is three-fold: 1.) The plasma provides highly energetic electrons which drive new reaction pathways via highly reactive atomic species, including H, O, and Cl. 2.) The plasma sputters chunks of the solid fuel material up into the flame where it is combusted, producing an agitated flame profile. 3.) The high voltage nsec pulses accelerate ionized species in the flame producing increased turbulence and mixing due to hydrodynamic effects (i.e., ionic winds) that improve the combustion. Full videos of this combustion process taken at a frame rate of 30 frames/*sec* are available in the Supplementary Information. Figs. 4b and c show the integrated intensity versus time plots obtained from the unfiltered (Fig. 4b) and 430nm-filtered (Fig. 4c) videos. Here, the integrated intensity is obtained by summing over all pixels in the CCD image. From these time-intensity plots, it is clear that the flame reaches its steady state magnitude around 15 s and is abruptly extinguished after the plasma is turned off at $t = 22$ s.

Fig. 5a shows the time series images of an end burner grain prepared with 50 % oxidizer. In this time series, the transient plasma (produced with 10 kHz pulses) is turned on at $t = 0$ s and turned off at $t = 12.4$ s. For this fuel mixture (i.e., 50 % oxidizer), the flame takes approximately 9.5 s to reach its steady state flame magnitude with the plasma on. After the plasma is turned off ($t = 12.4$ s), however, the flame continues to burn via self-sustained combustion until all the fuel is consumed. Nevertheless, a clear difference can be seen in the combustion with the plasma on. The CH emission ceases immediately after the plasma is turned off. Also, the flame profile becomes less agitated with lower surface area after the plasma is turned off. The complete videos of this combustion are available in the online Supporting Information documents. Figs. 5b and c show the integrated intensity-versus-time plots for the 50 % oxidizer fuel mixture. Here, the flame reaches its steady state flame magnitude in 9.5 s with the plasma on. After the plasma is turned off ($t = 12.4$ s), the

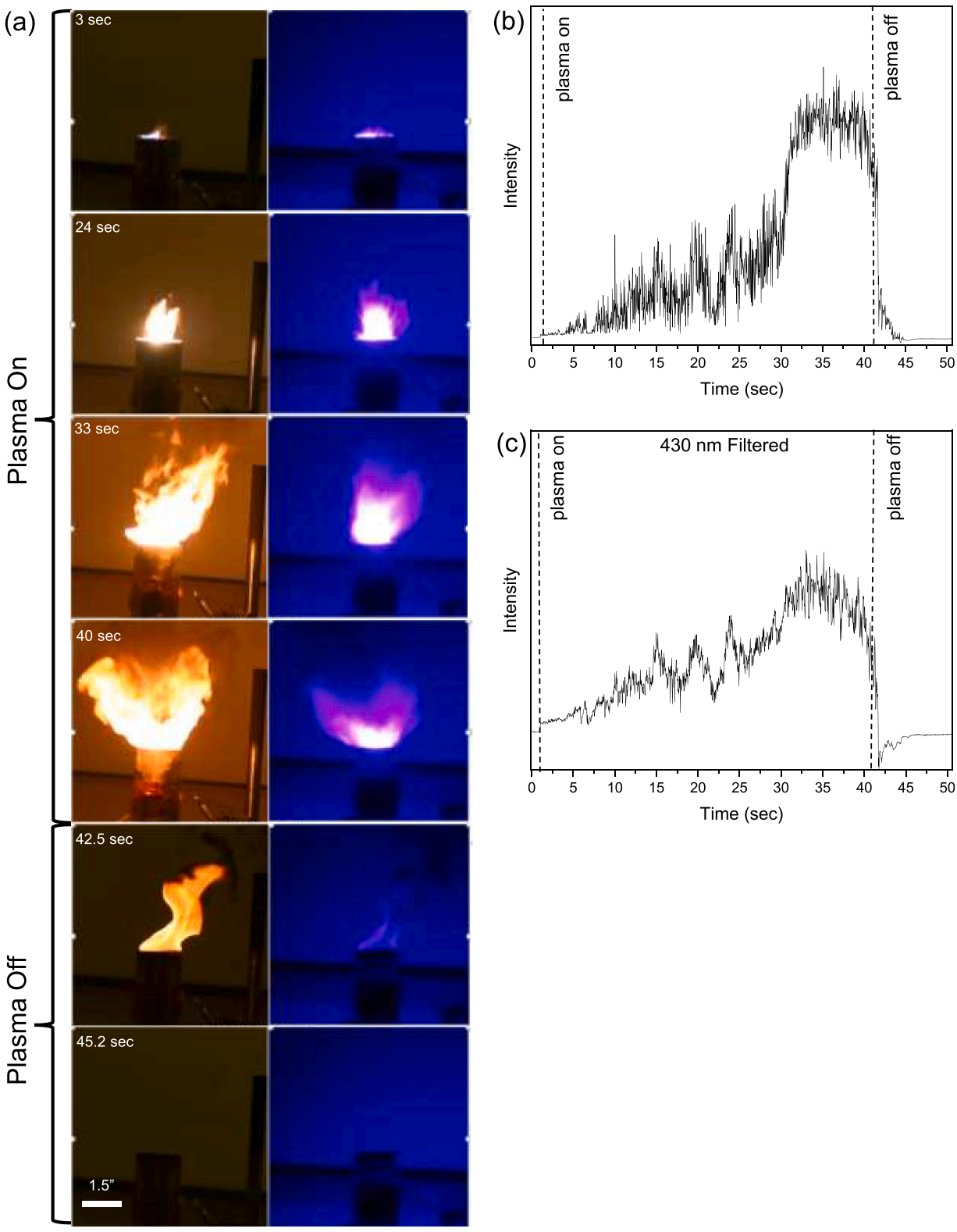

Fig. 3. (a) Time series images of solid rocket propellant with 25 % oxidizer. The transient plasma discharge (10 kHz repetition rate) was turned on at $t = 1$ s and turned off at $t = 41$ s. The right images were taken with 430 nm band pass filter (10 nm linewidth), which indicates the chemiluminescence produced by the short-lived CH combustion intermediate species. Complete videos are available in the online Supplemental Information. Integrated intensity versus time plots taken (b) without filter and (c) with 430 nm bandpass filter.

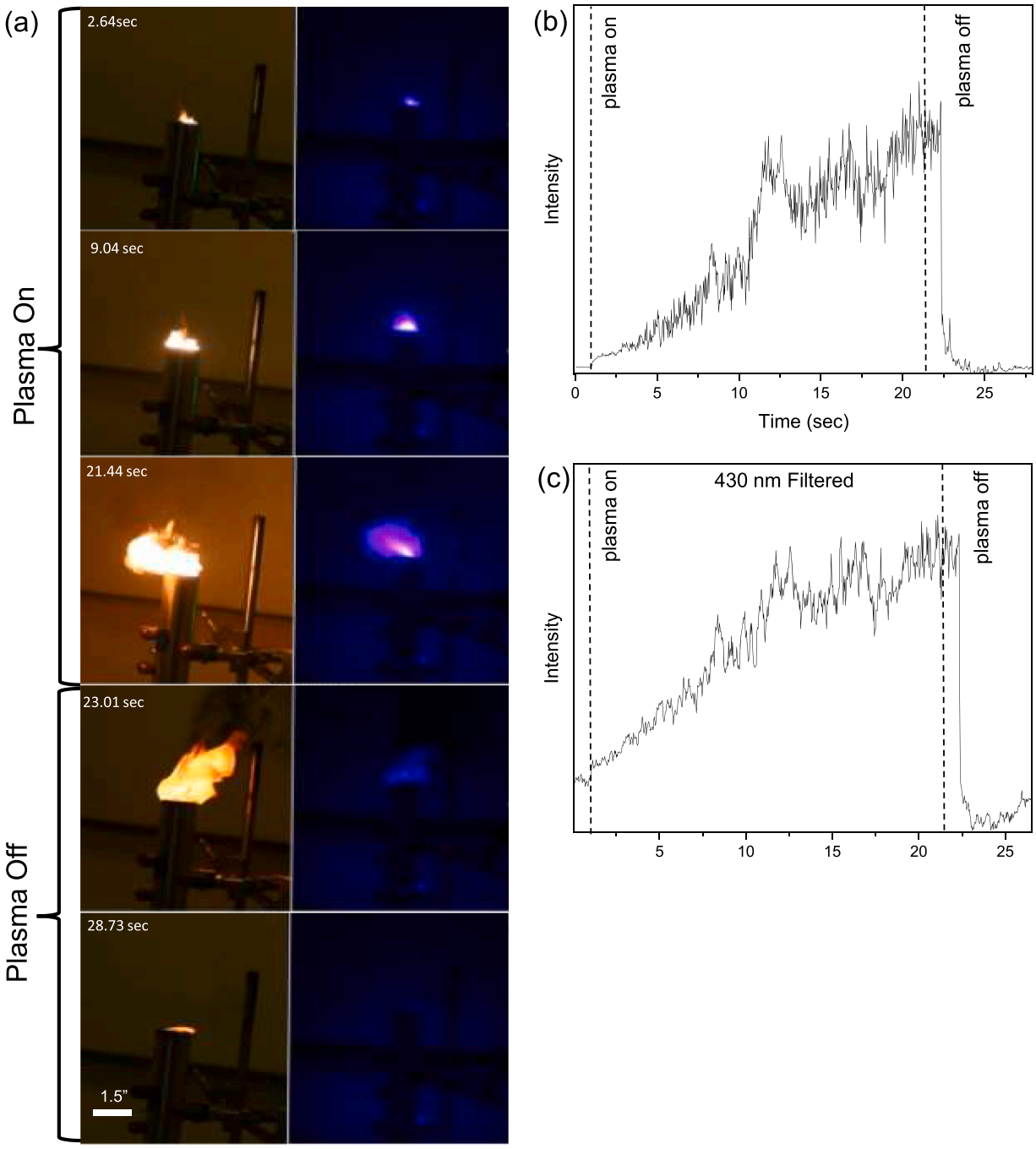

Fig. 4. Time series images of solid rocket propellant with 35 % oxidizer. The transient plasma discharge (10 kHz repetition rate) was turned on at $t = 1$ s and turned off at $t = 22$ s. The right images were taken with 430 nm band pass filter (10 nm linewidth), which indicates the chemiluminescence produced by the short-lived CH combustion intermediate species. Complete videos are available in the online Supplemental Information. Integrated intensity versus time plots taken (b) without filter and (c) with 430 nm bandpass filter.

unfiltered intensity (Fig. 5b) continues to remain high while the 430nm-filtered intensity (Fig. 5c) drops abruptly indicating a fundamental shift in the combustion mechanism. With this higher oxidizer content, the flame continues to burn in a self-sustained mode after the plasma is turned off, however, with markedly different CH emission (i.e., CH combustion pathways) largely absent.

Fig. 6 shows the time series images taken of the plasma-enhanced end burner grain with 65 % oxidizer. Here, the flame reaches its full steady state magnitude after approximately 17.5 s. After the plasma is turned off ($t = 26.1$ s), the flame continues to burn via self-sustained combustion until all of the fuel is consumed. Again, we see a clear difference in the flame profile and CH emission immediately after the plasma is turned off. Complete videos of this combustion are available in the Supporting Information. Figs. 6b and c show the corresponding total intensity-time plots for 65 % oxidizer which show that the full flame magnitude is reached within 17.5 s. As with the 50 % oxidizer fuel mixture, the unfiltered flame luminescence remains high after the plasma is turned off, while the 430nm-filtered intensity drops instantly indicating a dramatic shift in the combustion chemistry.

In conclusion, we demonstrate how nanosecond pulse transient plasma (NPTP) can enhance the combustion of solid rocket propellants. In this study, we fabricate end-burning propellant samples (i.e., grains)

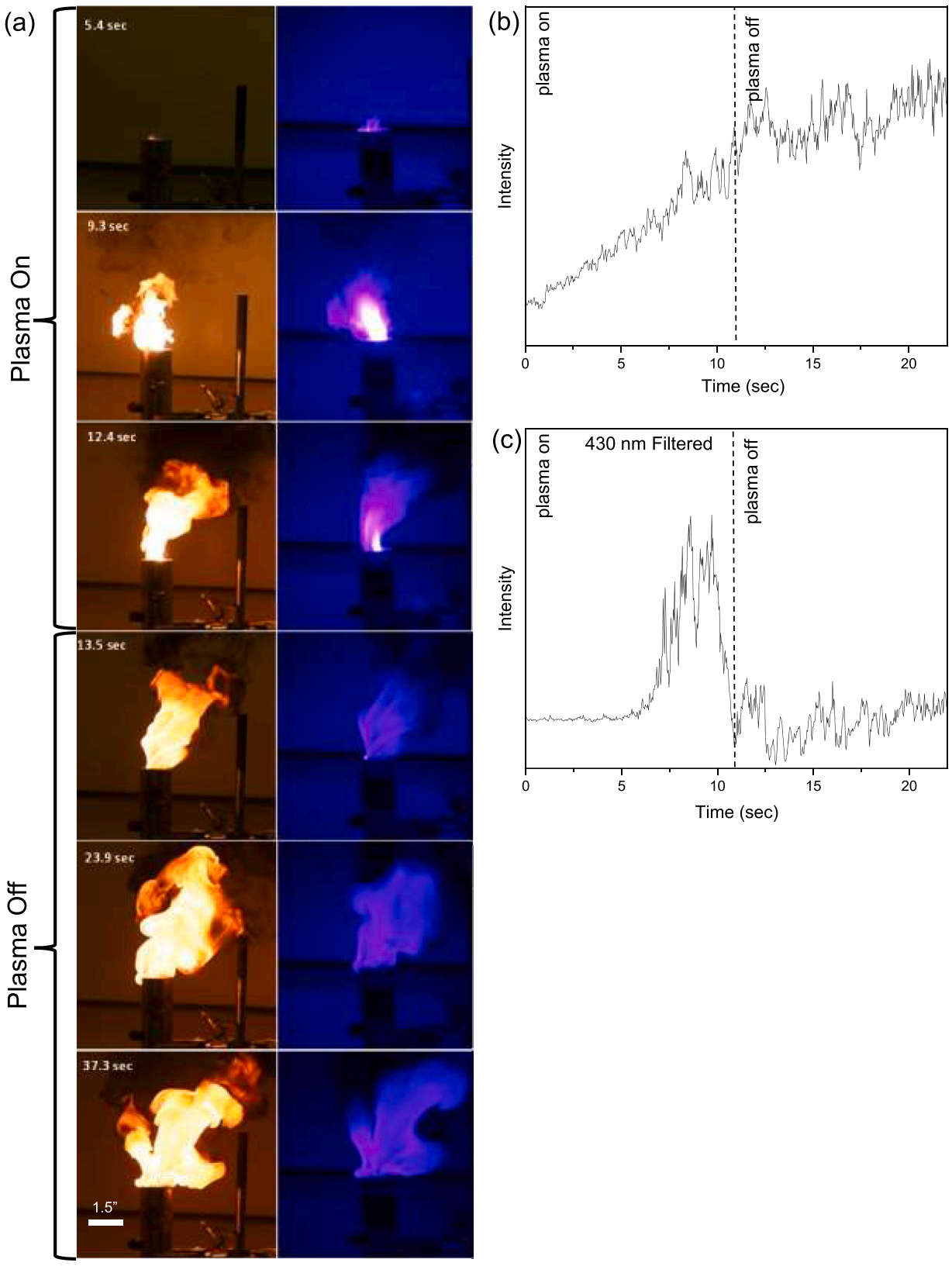

Fig. 5. Time series images of solid rocket propellant with 50 % oxidizer. The transient plasma discharge (10 kHz repetition rate) was turned on at $t = 0$ s and turned off at $t = 12.4$ s. The right images were taken with 430 nm band pass filter (10 nm linewidth), which indicates the chemiluminescence produced by the short-lived CH combustion intermediate species. Complete videos are available in the online Supplemental Information. Integrated intensity versus time plots taken (b) without filter and (c) with 430 nm bandpass filter.

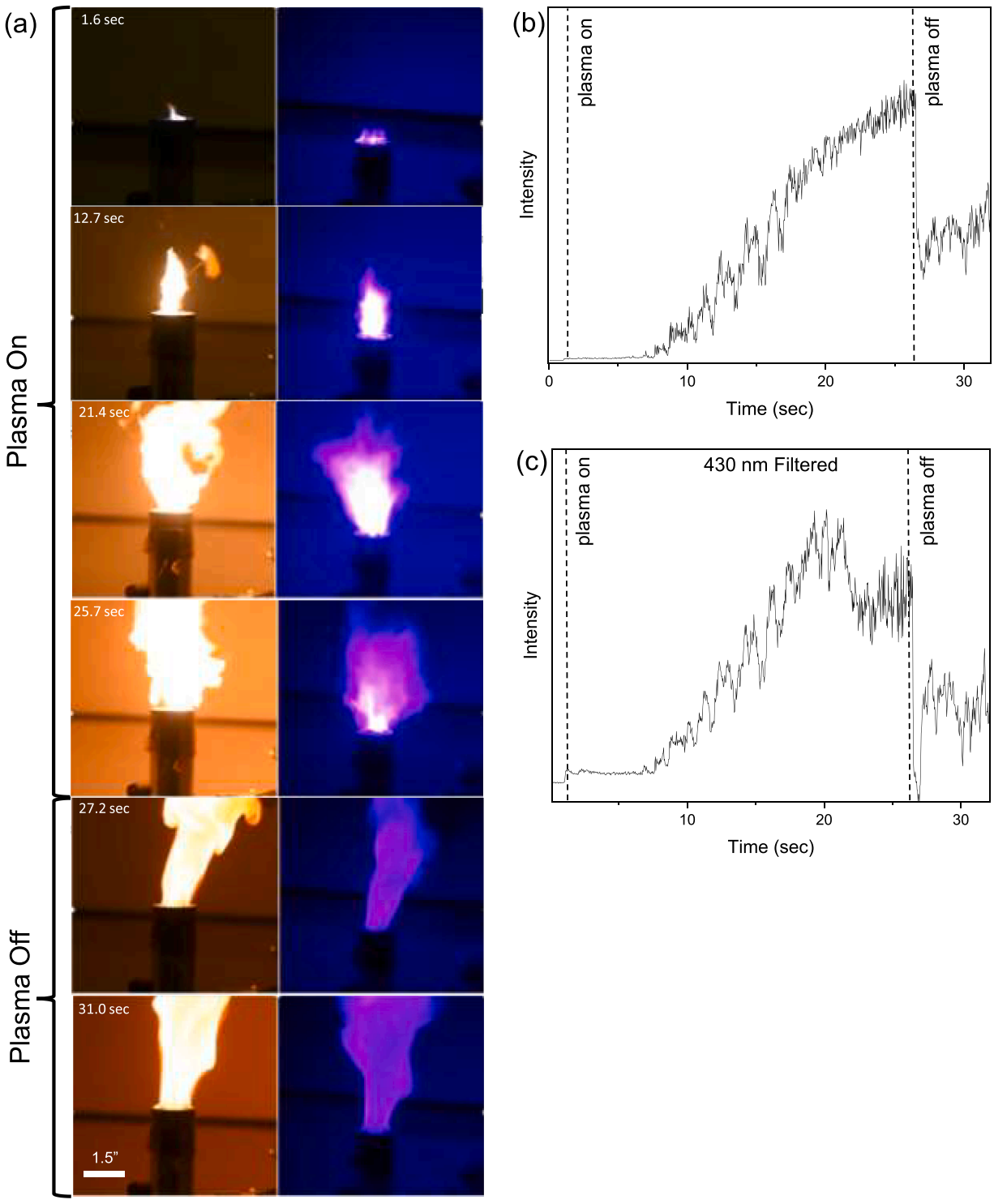

Fig. 6. Time series images of solid rocket propellant with 65 % oxidizer. The transient plasma discharge (10 kHz repetition rate) was turned on at $t = 1$ s and turned off at $t = 26.1$ s. The right images were taken with 430 nm band pass filter (10 nm linewidth), which indicates the chemiluminescence produced by the short-lived CH combustion intermediate species. Complete videos are available in the online Supplemental Information. Integrated intensity versus time plots taken (b) without filter and (c) with 430 nm bandpass filter.

with a co-axial center wire electrode using HTPB, IDP, MDI, and AP as the fuel, plasticizer, curative, and oxidizer, respectively. By applying high voltage nanosecond pulses (20 nsec) of 20 kV, we generate a streamer discharge that acts as an electronic control mechanism for the solid rocket propellant. We investigate various oxidizer mass fractions, including those classified as insensitive munitions (IM). Additionally, we employ real-time imaging to analyze the plasma formation, ignition process evolution, and the interaction between the plasma and the flame-propellant fuel. The enhancement mechanism can be attributed to three factors: 1.) The plasma introduces energetic electrons that facilitate new chemical pathways through highly reactive atomic species like H, O, and Cl, 2.) The plasma ejects solid fuel material up into the flame, resulting in a more dynamic combustion process, and 3.) The plasma induces increased turbulence and multi-scale mixing due to

hydrodynamics effects (ionic winds), thereby improving the combustion. This study serves as a proof-of-concept for electronically controlled solid rocket propellants. We have shown the ability to ignite and extinguish both 25 % and 35 % oxidizer propellant grains through the presence of plasma on the surface of the grain. For 50 % and 65 % oxidizer grains, combustion continued in a self-sustained manor after the plasma was removed, although at a slower rate and with markedly lower CH radical emission.

Novelty and significance statement

Electrical control of solid rocket propellants was proposed back in the 1960s and more recent studies have shown some ability to increase the specific impulse efficiencies with electrical solid propellants. The incorporation of "electronic" control over the burn rate enables the ability to adjust the power output of the solid propellant motor, opening up new possibilities for flight profiles that go beyond a predetermined option, like the standard boost-sustain profile. Here, we demonstrate the use of transient plasma to improve the control (and acceleration) of the combustion of solid rocket propellants for the first time. The transient plasma is a non-thermal plasma with extremely high ion densities and hot electron temperatures that drive new chemical pathways that are distinct from those of standard thermal equilibrium chemistry.

CRediT authorship contribution statement

Caleb Medchill: Data curation, Formal analysis, Methodology, Software, Writing – original draft, Writing – review & editing. **Armando A. Perezselsky:** Conceptualization, Investigation, Methodology, Writing – review & editing. **Andrew Cortopassi:** Project administration, Supervision, Writing – review & editing. **Alejandro L Briseno:** Project administration, Supervision, Writing – review & editing. **Chris Brophy:** Conceptualization, Project administration, Writing – review & editing. **Stephen B. Cronin:** Conceptualization, Project administration, Supervision, Writing – original draft, Writing – review & editing.

Declaration of competing interest

The authors declare that they have no known competing financial interests or personal relationships that could have appeared to influence the work reported in this paper.

Data availability

Data will be made available on request.

Acknowledgments

This research was supported by the Army Research Office (ARO) award no. W911NF-22-1-0284 (C.M.) and the National Science Foundation (NSF) award no. CHE-1954834 (S.C.).

Supplementary materials

Supplementary material associated with this article can be found, in the online version, at doi:10.1016/j.ast.2024.109107.

References

[1] P.J. Mayo, L.A. Watermeier, F.J. Weinberg, A.G. Gaydon, Electrical control of solid propellant burning, Proceedings of the Royal Society of London. Series A. Mathematical and Physical Sciences 284 (1965) 488–498.
[2] W.N. Sawka, M. McPherson, Electrical Solid Propellants: a Safe, Micro to Macro Propulsion Technology, in: 49th AIAA/ASME/SAE/ASEE Joint Propulsion Conference, 2013, https://doi.org/10.2514/6.2013-4168.
[3] S. J.Barkley, Microwave plasma enhancement of multiphase flames: on-demand control of solid propellant burning rate, Combust. Flame 199 (2019) 14–23.
[4] A. Kakami, Solid Propellant Microthruster Using Laser-Assisted Combustion, in: 40th AIAA/ASME/SAE/ASEE Joint Propulsion Conference and Exhibit, 2012, https://doi.org/10.2514/6.2004-3797.
[5] T. Ombrello, X. Qin, Y. Ju, A. Gutsol, A. Fridman, C. Carter, Combustion enhancement via stabilized piecewise nonequilibrium gliding arc plasma discharge, AIAA J. 44 (2006) 142–150.
[6] N. Anikin, I. Kosarev, E. Mintoussov, S. Starikovskaia, V. Zhukov, Plasma-assisted Combustion, Pure Appl Chem. Chimie Pure et Appliquee 78 (2006) 1265–1298.
[7] C. Cathey, J. Cain, H. Wang, M.A. Gundersen, C. Carter, M. Ryan, OH Production by transient plasma and mechanism of flame ignition and propagation in quiescent methane–air mixtures, Combust. Flame 154 (2008) 715–727.
[8] B. Wolk, A. Defilippo, J.-Y. Chen, R. Dibble, A. Nishiyama, Y. Ikeda, Enhancement of flame development by microwave-assisted spark ignition in constant volume combustion chamber, Combust. Flame 160 (2013) 1225–1234.
[9] L. Wu, J. Lane, N.P. Cernansky, D.L. Miller, A.A. Fridman, A.Y. Starikovskiy, Plasma-assisted Ignition below Self-ignition Threshold in Methane, Ethane, Propane and Butane-air Mixtures, P Combust Inst 33 (2011) 3219–3224.
[10] W. Fei, J.B. Liu, J. Sinibaldi, C. Brophy, A. Kuthi, C. Jiang, P. Ronney, M. A. Gundersen, Transient plasma ignition of quiescent and flowing air/fuel mixtures, IEEE T Plasma Sci 33 (2005) 844–849.
[11] R. Xing, S. Hammack, L. Tonghun, C. Carter, I.B. Matveev, Combustion dynamics of plasma-enhanced premixed and nonpremixed flames, IEEE T Plasma Sci 38 (2010) 3265–3271.
[12] Z. Yin, A. Montello, C.D. Carter, W.R. Lempert, I.V. Adamovich, Measurements of temperature and hydroxyl radical generation/decay in lean fuel–air mixtures excited by a repetitively pulsed nanosecond discharge, Combust. Flame 160 (2013) 1594–1608.
[13] B. Shukla, V. Gururajan, K. Eisazadeh-Far, B. Windom, D. Singleton, M. A. Gundersen, F.N. Egolfopoulos, Effects of electrode geometry on transient plasma induced ignition, J Phys D Appl Phys 46 (2013) 205201.
[14] S. Biswas, Assessment of Spark, Corona, and Plasma Ignition Systems for Gasoline Combustion, in: Proceedings of the ASME 2020 Internal Combustion Engine Division Fall Technical Conference, 2020, https://doi.org/10.1115/ICEF2020-3034.
[15] D. Alderman, C. Tremble, S. Song, C. Jiang, Plasma kinetics study of a repetitive 10-nsec pulsed plasma ignition for combustion, in: IEEE Pulsed Power & Plasma Science Conference, 2019, https://doi.org/10.1109/PPPS34859.2019.9009621.
[16] B. Bihari, M.S. Biruduganti, R. Torelli, D. Singleton, Performance characterization of alternative ignition systems using optical tools in natural gas engines, in: Proceedings of the ASME 2018 Internal Combustion Fall Technical Conference, 2018, https://doi.org/10.1115/ICEF2018-9704.
[17] D. Alderman, C. Tremble, C. Jiang, J.M. Sanders, Initial evaluation of pulse risetime on transient plasma ignition for combustion, in: Proceedings of the 2018 IEEE International Power Modulator and High Voltage Conference, 2018, https://doi.org/10.1109/IPMHVC.2018.8936811.
[18] D. Pineda, The role of hydrodynamic enhancement on ignition of lean methane-air mixtures by pulsed nanosecond discharges for automotive engine applications, Combust. Sci. Technol. 189 (11) (2017) 2023–2037.
[19] J. Choe, W. Sun, T. Ombrello, C. Carter, Plasma assisted ammonia combustion: simultaneous NOx reduction and flame enhancement, Combust. Flame 228 (2021) 430–432.
[20] Q. Lin, Y. Jiang, C. Liu, L. Chen, W. Zhang, J. Ding, J. Li, Controllable NO emission and high flame performance of ammonia combustion assisted by non-equilibrium plasma, Fuel 319 (2022) 123818.
[21] Y. Tang, D. Xie, B. Shi, N. Wang, S. Li, Flammability enhancement of swirling ammonia/air combustion using AC powered gliding arc discharges, Fuel 313 (2022) 122674.
[22] D.R. Singleton, J.O. Sinibaldi, C.M. Brophy, A. Kuthi, M.A. Gundersen, Compact pulsed-power system for transient plasma ignition, IEEE T Plasma Sci 37 (2009) 2275–2279.
[23] F. Wang, A. Kuthi, C. Jiang, M. Gundersen, Pseudospark based pulse forming circuit for plasma ignition system, in: Digest of Technical Papers. PPC-2003. 14th IEEE International Pulsed Power Conference (IEEE Cat. No.03CH37472), 2003.
[24] D. Singleton, C. Cathey, A. Kuthi, M. Gundersen, Applications of Power Modulator Technology to Ignition and Combustion, in: 28th International Power Modulator Symposium/2008 High Voltage Workshop, 2008, https://doi.org/10.1109/IPMC.2008.4743608.
[25] F. Wang, C. Cathey, A. Kuthi, T. Tang, H. Chen, M.A. Gundersen, Pseudospark-Based Power Modulator Technology for Transient Plasma Ignition, in: Conference Record of the 2006 Twenty-Seventh International Power Modulator Symposium, 2006, https://doi.org/10.1109/MODSYM.2006.365256.